Tribology International 170 (2022) 107504

Contents lists available at ScienceDirect

Tribology International

journal homepage: www.elsevier.com/locate/triboint

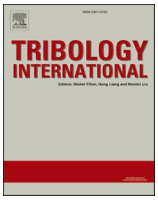

An insight into the effect surface morphology, processing, and lubricating conditions on tribological properties of Ti6Al4V and UHMWPE pairs

Kamil Leksycki [a], Eugene Feldshtein [a], Radosław W. Maruda [a], Navneet Khanna [b], Grzegorz M. Królczyk [c,*], Catalin I. Pruncu [d,e,**]

[a] Faculty of Mechanical Engineering, University of Zielona Gora, 4 Prof. Z. Szafrana str., 65-516 Zielona Góra, Poland
[b] Advanced Manufacturing Laboratory, Institute of Infrastructure Technology, Research and Management, Ahmedabad 380008, India
[c] Opole University of Technology, 76 Proszkowska St., Opole 45-758, Poland
[d] Department of Mechanical Engineering, Imperial College London, Exhibition Rd., London, UK
[e] Design, Manufacturing & Engineering Management, University of Strathclyde, Glasgow G1 1XJ, Scotland, UK

ARTICLE INFO

Keywords:
Ti6Al4V alloy - UHMWPE pair
Near-dry cutting conditions
Surface topography
Friction and wear behavior
SBF environment

ABSTRACT

The effects of surface topography, processing, and environment conditions during tribological contact between Ti6Al4V titanium alloy and UHMWPE friction pairs were systematically evaluated. Hence, in this research the polyethylene samples (blocks) having a constant surface roughness were rubbed against counter-bodies (rollers) made of titanium alloy with different roughness of surfaces. The counter-samples were manufactured using either dry machining and/or minimum quantity lubrication (MQL) conditions. Such cutting conditions are harmless to humans and the environment. Simulated body fluid (SBF) and distilled water was used to simulate the tribological trials. We have noted that the lubricant applied to protect the integrity of machined parts, the rollers, have only minor impact on the tribological features of the friction pairs tested. Further, the samples produced with dry machining demonstrated a slightly lower momentary friction coefficient and temperature. In contrast, the MQL method enable reduced friction surface and significant wear accumulation. Further, it was found that the minimum and maximum values of the *Sa* texture parameter associated to tribological parameters do not exceed 21% and 4%, when is used dry and MQL methods, respectively. Nevertheless, the distilled water revealed a much better wear resistance when comparing to SBF, and the later one trigger as well as an accentuated wear progress with different patterns. The results of the study are important in the design of new biomedical components produced by finish turning.

1. Introduction

The surface integrity of materials used in the medical purposes are affected mainly by the wear process [1,2]. Nowadays, the implant introduced on the human body allows extending considerably the life expectancy [3–5]. There are many movable joints introduced on the human body (i.e. ankle, arm, elbow, wrist, skull or tooth) [6]. Initially, after joint replacement, implants perform their biomechanical function very well [7]. However, during longer life expectancy, regardless of the material used, they wear out, which is inevitable [6]. As a result of wear, toxic metal ions are transmitted through human body by the synergistic mechanism of combined friction and corrosion, which trigger serious and undesired reactions [8–11] as well as implant relaxation [12].

The ultra-high molecular weight polyethylene (UHMWPE) represents a common material designed as biomedical part. It results from its favorable tribological and mechanical properties and chemical stability [13]. UHMWPE is successfully used in orthopedic areas, e.g. as a substitute for artificial human joints, due to reduced friction coefficient and acceptable biocompatibility with the human body [14]. Another material that is most used for implants is Ti6Al4V titanium alloy [4,15]. It is characterized by favorable mechanical attributes and a good combination between biocompatibility and corrosion resistance [16,17]. The artificial hip joints contain the combination of Ti6Al4V alloy and UHMWPE which provide an appropriate system [18].

A series of tribological studies have been devoted to biomedical friction pairs under different lubrication conditions. Chen et al. [19]

* Corresponding author.
** Corresponding author at: Department of Mechanical Engineering, Imperial College London, Exhibition Rd., London, UK.
E-mail addresses: g.krolczyk@po.opole.pl (G.M. Królczyk), Catalin.pruncu@gmail.com, catalin.pruncu@strath.ac.uk (C.I. Pruncu).

https://doi.org/10.1016/j.triboint.2022.107504
Received 23 November 2021; Received in revised form 27 January 2022; Accepted 20 February 2022
Available online 25 February 2022

examined the performance of different biocompatible alloys (316 L stainless steel against Ti6Al4V titanium alloy) for their corrosion and tribocorrosion resistance using artificial sea water with Al_2O_3 ceramic. Friction accelerated the corrosion and material's wear was higher in sea water than in pure water. Sonekar and Rathod [20] compared the tribological behavior of 316 L stainless steel manufactured as a disc-shaped sample and Ti6Al4V titanium alloy as ball. Ti6Al4V alloy demonstrated reduced wear rate compared with 316 L steel. Machining characteristics and cooling type were evaluated to detect the amount of wear produced by the "Ti6Al4V alloy CoCrMo alloy" simulated in harsh environment saline composition made of 0.9% NaCl in distilled water by Bruschi et al. [21]. There was noted that cryogenic condition are better conditions, when comparing to dry machining, showing lower friction coefficient and almost no metal debris there. Pure titanium CP-Ti, titanium alloys Ti6Al4V and Ti-5Al-2.5Fe were verified by Choubey et al. [22] to understand their tribological behavior using Hanks simulated body fluid. A ball made of bearing steel was used as a counter-body. The dominant mechanism of wear was tribomechanical wear. The lowest coefficient of friction was registered for titanium alloy Ti-5Al-2.5Fe, for other alloys it was 1.5–2 times higher. Allen et al. [23] analyzed the wear of UHMWPE cooperating with Ti6Al4V titanium alloy. Surface modification were designed using nitrogen ions implanted either manufacturing UHMWPE surface layer and/or in the surface layer of titanium alloy in order to improve the tibological properties and the resistance to air oxidation [24]. The research was carried out under dry condition and distilled water lubrication. The presence of distilled water and lower surface roughness of friction pair elements ensured a decrease of friction coefficient. No polyethylene was observed on titanium alloy surface. Bian et al. [25] studied biocompatibility, biotribological properties and wear debris morphology of UHMWPE and ULWPE (ultra--low-wear) at contact with CoCr alloy. The bovine serum lubricant was used when testing. ULWPE showed better abrasion resistance when comparing to UHMWPE. The worn surfaces morphology showed similar wear mechanisms for both materials, i.e.: adhesion wear, abrasive wear and fatigue wear. Wang et al. [26] researched the intensity of friction and wear of UHMWPE containing glass and carbon fibers in dry and distilled water environments. AISI 52100 steel manufactured with low surface roughness, $Ra = 0.1$ μm and 0.3 μm was used as a counter-body. It was found that the coefficient of friction in the environment with distilled water was lower compared to dry friction. Also, they noted as beneficial presence of a thin water layer located at the interface of metal and polymer which in turn prevents adhesion wear and the filling of polyethylene with fibers additionally reduced the coefficient of friction. Barret et al. [27] investigated the effect of surface roughness and friction speed on tribological behavior of UHMWPE − stainless steel pair. Melting of polyethylene was observed at higher surface roughness and sliding speeds. At higher speeds it was observed that the influence of roughness on the wear intensity was decreasing. Wear debris were observed on the stainless-steel surface. Xiong et al. [28] studied friction and wear properties of UHMWPE against ion implanted Ti6Al4V alloy in the environment of distilled water. On the surface of titanium alloy, the graded titanium oxide-titanium nitride film was formed. The surface engineering, with ion implantation, for the UHMWPE can lead to as much as 5 times lower friction coefficients and up to 40 times reduction of wear amount. Further, the surface of Ti6Al4V alloy can reveals numerous deep grooves without ion implantation, however after modifying the surface with this engineering treatments almost no defect are identified. Langhorn et al. [29] analyzed wear of HDPE polyethylene in contact with microtextured CoCrMo alloy. The studies were carried out in the environment of bovine serum. Compared to the polished CoCrMo surface, the microtextured surface ensured reduction of polyethylene wear by over 50%.

There is almost no information concerning the influence of contact surface processing conditions i.e. surface topography and also influence of cooling conditions on the interaction of titanium alloys with polyethylene. However, the processing conditions affect the surface topography [30], tribological properties [31] or corrosion resistance [32]. The heat treatment was applied by Sartori et al. [33] to improve the integrity of surface condition of Ti6Al4V; then this treatment was followed by machining in dry and cryogenic cooling conditions. Compared to dry machining, cryogenic machining provides less surface defects, but the deterioration of surface topography was noted. A detailed examination was provided by Zhang and Liu [34] on the surface topography generated by dry finish turning of Ti6Al4V alloy. They indicated that the *Ra* and *Rz* parameters are affected majorly by the higher amount of feed rate. Further, Sun et al. [35] applied dry machining on the Ti-10 V-2Fe-3Al alloy to detect its surface integrity performances. It was revealed that a higher cutting speed can reduce the number of defects on the machined surface. In mean time, they noted that a better surface condition can be achieved with smaller feeds rate. Other studies, on the machinability of Ti-5553 alloy were performed by Sun et al. [36]. They found the best roughness condition applying MQL machining process while wet conditions and cryogenic cooling were slightly detrimental.

To further improve the state of art, this paper is focused to fundamentally describe the effect of the surface topography and processing conditions on the tribological and wear behavior of Ti6Al4V titanium alloy and UHMWPE pairs subjected to different environment, i.e. distilled water and simulated body fluid (SBF). It allows the simultaneous analysis of surface features and environment effect on implants life expectancy. The obtained research results are extremely important from the point of view of designing new biomedical components used for human implants produced by finishing turning.

2. Materials and methods

The rollers (counter-bodies) were made of Ti6Al4V titanium alloy. According to ISO 5832–3:2016 this material is characterized by elastic modulus of 110–114 GPa, a tensile strength of 960–970 MPa, yield strength of 850–900 MPa, fatigue strength of 620–725 kJ/m^2. Samples (blocks) were made of ultra-high molecular weight of polyethylene (UHMWPE). The density of UHMWPE used is 0.93 g/cm^3, while the average molecular weight is ~5 Mio. g/mol. It has a modulus of elasticity $\geq$ 700 MPa, tensile strength $\geq$ 30 MPa, yield strength $\geq$ 17 MPa, fatigue strength $\geq$ 170 kJ/m2, softening temperature ~80 °C and melting temperature 130 − 140 °C.

The rollers were processed using a DMTG CKE6136i CNC lathe. Further, the lathe cutter was equipped with a tool holder (CoroTurn SDJCR 2525 M 11) and an insert (CoroTurn DCMX 11 T3 04-WM 1115) in order to manufacture the samples. A GC1115 insert material coated with cemented carbide (S group as per ISO 513:2012 standard) and (Ti, Al)N + $(Al,Cr)_2O_3$ coating which were produced under PVD method were used. A constant depth of cut, equal to 0.5 mm, was used that corresponds to medium finish machining. It can be obtained usually imposing a cutting speed of 37.5 − 125 m/min corroborated with a feed rate of 0.05 − 0.4 mm/rev. Near-dry cutting conditions were applied using either dry conditions and/ or minimum quantity lubrication (MQL), that ware described by Krolczyk et al. [37]. Parameter Space Investigation (PSI) strategy was implemented to design the test plan [38] and the minimum and maximum values of surface roughness parameters were determined.

Optical profilometry under Sensofar S Neox 3D machine were employed to detect the surface machined topography. Measurement results were analyzed using Mountains Maps Premium 7.4 software. For the analysis, the most widely used 3D surface roughness parameter *Sa* (arithmetical mean height of the scale limited surface), *Ssk* (Skewness) and *Sku* (Kurtosis) as high parameters and hybrid parameters *Sdq* (root mean square (RMS) surface slope) and *Sdr* (developed interfacial area ratio) was chosen; according to ISO 25178–2:2012. The use of multiple combinations, of roughness parameters, offers effective solutions to describe the surface evolution subjected to different machining operation. The parameter correlation *Ssk* and *Sku* enable creating *Ssk-Sku*

topological map which leads to an appropriate assessment of the distribution of surface irregularities. They depend mainly of high peaks and deep pits characteristics [39]. Further, the parameter correlation *Sdq* and *Sdr* enables creating *Sdq-Sdr* (hybrid) topological maps used for the identification of defects and probably some discrepancies on the surface. It can be used as well as to reveals some microgeometry and structural changes generated by the wear processes [40]. Based on the results obtained for the analyzed cooling conditions, minimum and maximum *Sa* values of the tested rollers were determined. The minimum *Sa* value of the surface treated was 0.36 μm for both dry and MQL conditions, while the maximum values were *Sa* = 2.24 μm and *Sa* = 1.84 μm, respectively. The polyethylene samples were processed by grinding to obtain the surface roughness parameter *Sa* = 0.4 μm. The widths of the wear trace were measured using the Dino Lite AM7013MZT digital universal microscope which has very good accuracy, about 1 μm. The patterns morphology produced by the surfaces interacted as a friction pair was examined using the digital optical microscope Zeiss Axio Observer A1m.

Tribological tests were carried out with the use of the self-made A-135 tester, which allows to conduct experiments in the "block-on-disc" system under concentrated load conditions. In this system, the UHMWPE block remained stationary while the Ti6Al4V alloy roller rotated at a constant speed. This is similar activity pattern to the hip joints work, where the femoral head makes movements relative to the acetabulum [4]. The rollers tested were of 50 mm diameter and 15 mm width, and the blocks had the width of 10 mm, height of 14 mm, and length of 20 mm. At the center of the side wall of the block, there was drilled a hole to accommodate a thermocouple for registering the thermoelectric force. It was placed at a 2 mm distance from the friction surface.

The applied method enables the simulation of various operating conditions, e.g. at high temperature, high friction speeds or high load [41]. Distilled water and simulated body fluid (SBF) were used as lubricants. The chemical composition of SBF is shown in Table 1 and is close to the chemical composition of human blood plasma. The SBF fluid solution had a pH in the range of 7.2–7.4. In vitro studies conducted in the presence of SBF may result in the formation of an apatite layer on the metal surface, which is considered to be a factor affecting the ability to connect bones [42]. Distilled water was considered as base fluid for the SBF. The use of different research conditions, which are due to different masses and movement intensity of humans or the different temperatures that surround their bodies was described for tribological testing of biomaterials. The parameters of the tribological tests were determined on the basis of preliminary tests. During the tribological tests the lubricant was fed with the rate of 30 drops/min, which provided constant non-intensive lubrication (as occurs in the human body). A constant 500 N load collaborated with a friction speed of 0.5 m/s were applied. The friction cycle time was set to 30 min. Due to the varying the loads and intense work of artificial human joints, such loads, the speed and time of the friction cycle were used to ensure that the temperature in the friction zone would be close to but not exceed the softening temperature of UHMWPE. In the tests, the measurements were repeated 3 times, and the standard deviation did not exceed 5%. Measurement uncertainty was controlled according the method A of ISO and VDA5 recommendations.

Table 1
Chemical composition of SBF [43].

Reagents	SBF solution, amount (g l^{-1})
NaCl	8.035
KCl	0.225
$CaCl_2$	0.292
$NaHCO_3$	0.355
Na_2SO_3	0.072
$K_2{\cdot}HPO_4.3\ H_20$	0.292
$MgCl_2.6\ H_2O$	0.311
1 M HCl	39 ml
Tris	6.118
1 M HCl	0–5 ml

During the tests, changes in the momentary friction coefficient $\int_{ch}$ as well as changes in temperature *T* in the friction zone over time were registered. Volumetric wear I_v and wear rate I_{v0} of the samples tested were determined using measurements of the width of wear traces. Calculations were fulfilled using equations [44]:

- Momentary coefficient of friction μ_{ch} $\int_{ch}$:

$$\mu_{ch} = \frac{2M_t}{P_o D_0} \tag{1}$$

where: M_t – moment of friction, Nm; P_o– load, N; D_0 – roller diameter, mm.

- Volumetric wear I_V:

$$I_V = \frac{D_o^2 l_p}{8}\left\{2arcsin\left(\frac{b}{D_0}\right) \quad -sinsin \quad \left[2arcsin\left(\frac{b}{D_o}\right)\right] \quad \right\} \tag{2}$$

where: l_p– block width, mm; *b* – average width of wear trace, mm.

- Wear rate I_{V0}:

$$I_{Vo} = \frac{I_V}{L} \tag{3}$$

where: *L* – friction path.

Fig. 1 presents and overview with the entire experiment set-up used in this research. The lathe machine was used to produce the samples. Then, the samples were evaluated for roughness with a 3D profilometry. Once the surface was certified as statistical uniformly the samples were subjected to tribological trials. Finally, the worn surface was analyzed for their microstructure characteristics.

3. Results and discussion

Details of 3D topography, of the rollers surface submitted to finish turning imposing dry and MQL machining conditions were depicted in Fig. 2. Here, the main characteristics correlated were minimum and maximum *Sa* values. The analysis surface with *Sa* parameters reveals some regular small feed traces that appear as peaks and valleys and also irregularly spaced stickers, morphologies indicated also in Leksycki and Feldshtein [45]. They may occur as a result of adhesive chip sticking to the machined surface. Krolczyk et al. [39] found that stickers which are cut off during friction process are susceptible to wear formation and acceleration of defect. Otherwise, the maximum *Sa* parameters offer information about formation of feed traces over the surface which has regular high peaks and valleys, morphology which was also highlighted in Bordin et al. [46]. In the case of the minimum *Sa* values, the changes on the surfaces reach 13 μm for dry machining and 9 μm for MQL, and for the maximum *Sa* values, 16 and 18 μm, respectively.

Fig. 3 presents the material ratio curves together with distributions of peak height associated to the rolls surfaces in respect to the minimum and maximum values of *Sa* parameter after finish turning in dry and MQL conditions. There, the minimum *Sa* for either cooling conditions has a mixed directionally nature for the machined surface peaks, while for the maximum *Sa* it is periodic.

Fig. 4 shows the *Sku-Ssk* map and the *Sdq-Sdr* (hybrid) map of the surface of the rolls with the minimum and maximum *Sa* values after finish turning in dry and MQL conditions. By analyzing the *Sku-Ssk* map (Fig. 4a), and comparing the area with the maximum sizes, for the minimum *Sa* values it is revealed a slightly decrease in the *Ssk* parameters. The dry cutting surfaces generated with a low value of the *Sa* parameter are characterized by deeper valleys. The value of the *Sku* parameter below "3" number proves the regular shape of the surface [39]. Thus, the dry cutting which generated surface with low value *Sa* parameter forms irregular surfaces. It is characterized by numerous

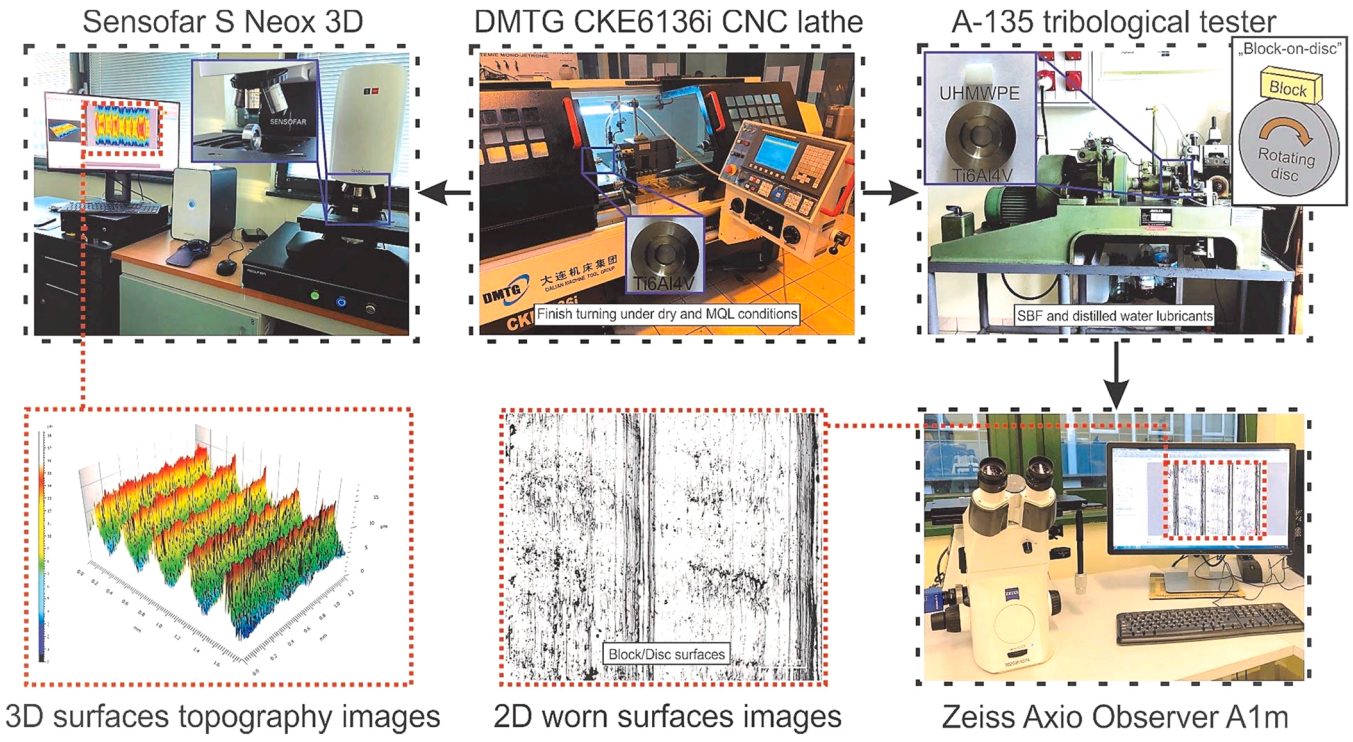

Fig. 1. Experimental setup to produce the samples and evaluation.

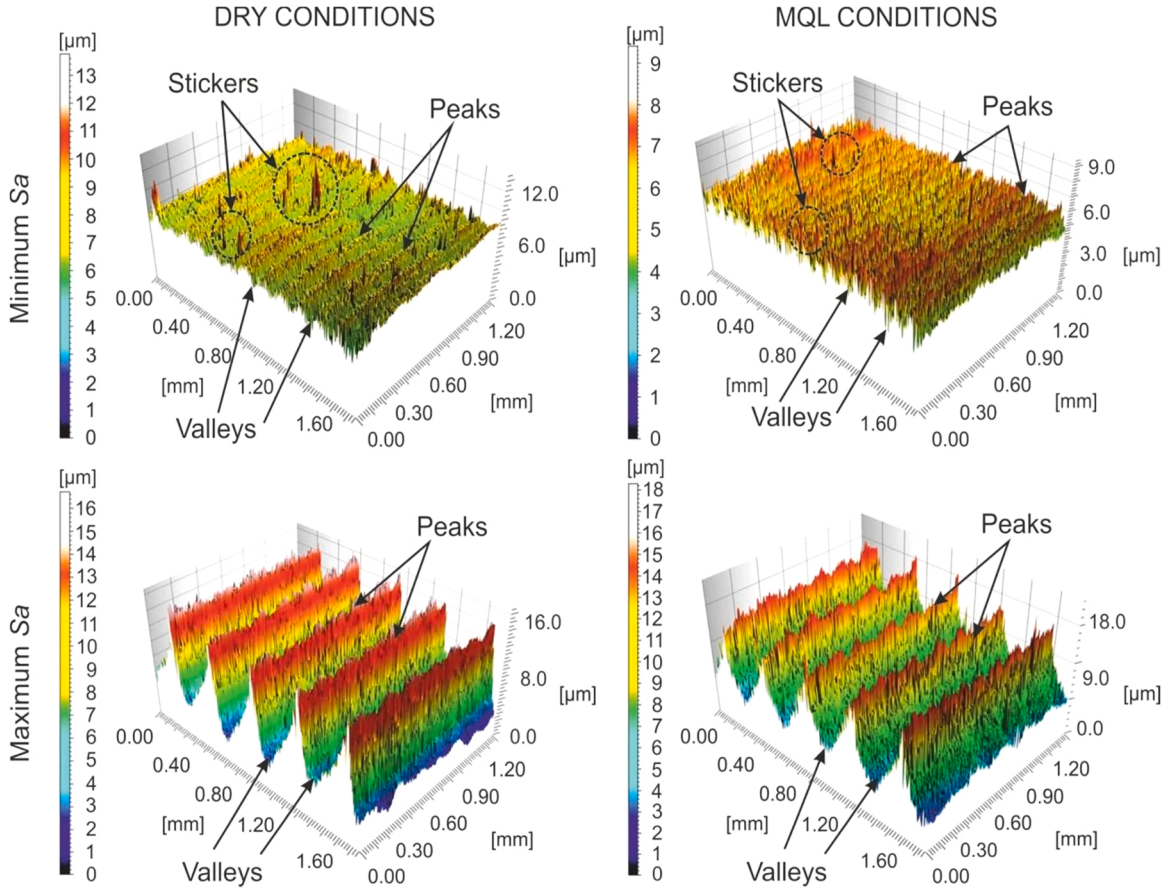

Fig. 2. The 3D topography of the rollers surface made of Ti6Al4V alloy.

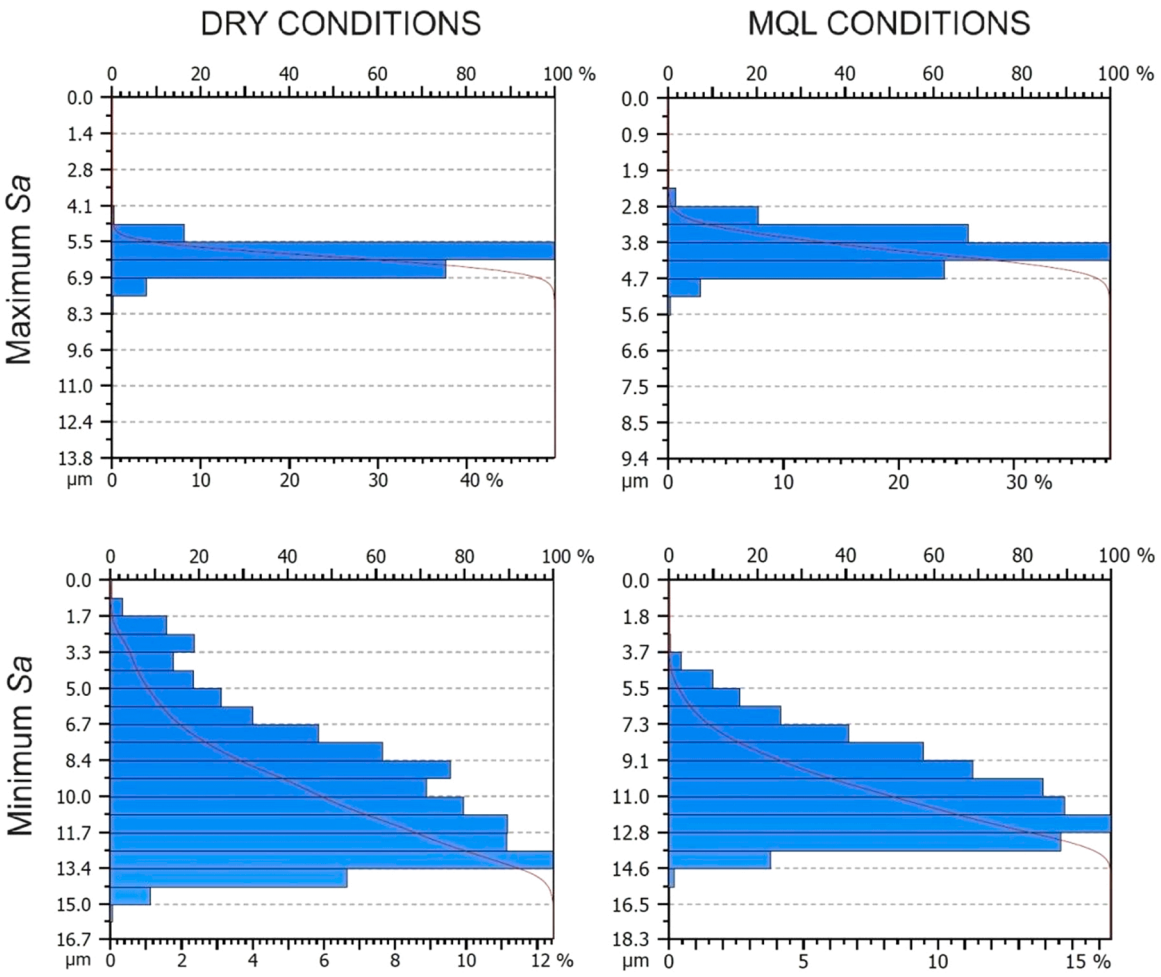

Fig. 3. Patterns of material ratio curves and peak height distributions for the rollers surface made of Ti6Al4V alloy.

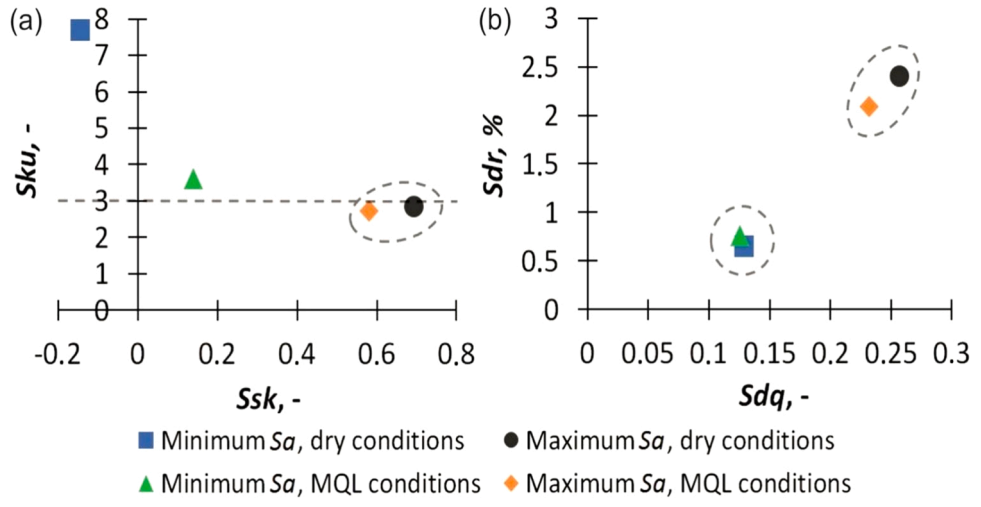

Fig. 4. *Sku-Ssk* map (a) and *Sdq-Sdr* map (b) of the rollers surface made from Ti6Al4V titanium alloy.

single sharp and high peaks (see details in Fig. 2). Niemczewska-Wójcik [47] showed that from the tribological point of view, sharp peaks in the initial stage of friction will be cut off. By analyzing the *Sdq-Sdr* map (Fig. 4b) we understood that the lower surface roughness value is achieved, regardless of the cutting conditions. Further, it can be seen a reduction in the *Sdq* and *Sdr* hybrid parameters, associated to a smaller number of surface defects, injuries and machining discrepancies [40].

Fig. 5 depicts the variation in friction coefficient for the duration of trial. They are provided for various surface having different minimum and maximum *Sa* values caused by different processing conditions in the presence of distilled water (Fig. 5a). For maximum *Sa* values and dry turning conditions, the momentary coefficient of friction was the smallest and decreased over time. Such changes were associated to increasing gradually of area of contact between the sample and the

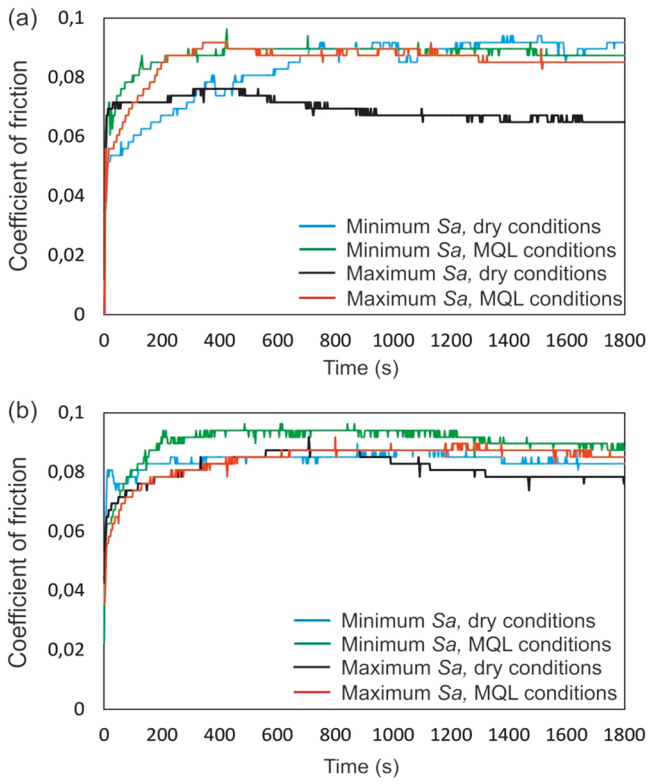

Fig. 5. Changes in friction coefficients over time in the presence of (a) distilled water and (b) SBF.

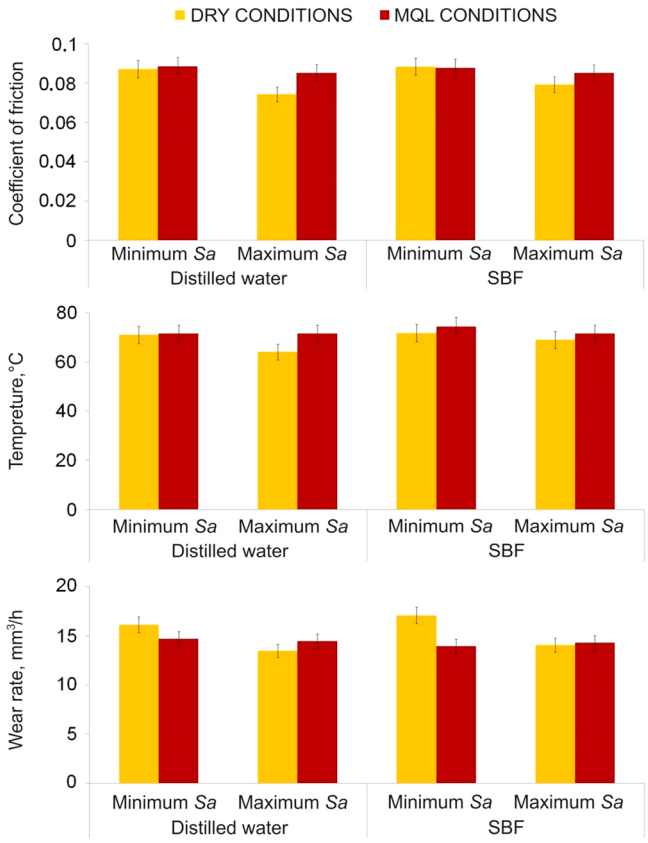

Fig. 6. The influence of processed conditions and lubricant on tribological properties tested.

counter-body and a decrease in actual pressure. Similar changes were observed in the case of SBF presence (Fig. 5b). The highest momentary coefficient of friction was recorded for minimum *Sa* values and MQL cooling conditions with the presence of SBF. Moreover, it was found that the running-in time of the tested friction pairs can be determined as short.

The influence of friction surfaces processing and lubrication conditions on the values of momentary friction coefficient, temperature and wear rate is shown in Fig. 6. It was found that the type of lubricant do bring only minor variation on tribological properties. Compared to the minimum *Sa* values, the maximum *Sa* values provide more favorable results. For minimum *Sa*, a slight reduction in momentary friction coefficient and temperature was observed for dry machining, nevertheless a higher reduction in wear rate was achieved using MQL. For maximum *Sa*, a reduction of the analyzed tribological properties was achieved for dry machining compared to MQL. The changes of the parameters tested are presented in Tables 2 and 3. For surfaces processed under dry machining, for minimum *Sa* compared to maximum *Sa*, parameter changes on an average of ~21% were obtained. On the other hand, for rollers processed under MQL conditions, parameter changes of ~4% were obtained.

When analyzing the tribological properties of the friction pair "Ti6Al4V alloy–UHMWPE", the properties of the materials and the influence of temperature occurring in the friction zone should be considered. Under significant loads, the average temperature of the contact surface approaches the softening temperature of polyethylene. It influences the progression of the friction process because particles of the melted material penetrate into the micro-irregularities on the surface of titanium alloy rollers, as shown by Baena and Peng [48].

The worn surfaces of samples and counter-bodies treated under dry processing conditions and MQL conditions, as well as surface features caused by various physical phenomena are shown in Figs. 7 and 8.

The analyses of tribological behavior of friction pairs require considering the common interaction of the temperature in the friction zone and the properties of the materials tested. Dong et al. [49] indicated that the greater temperature on the friction knot is responsible for the risk of wear processes, creep and degradation of UHMWPE. Under high loads, the friction temperature is close to the softening temperature of polyethylene. Taking into account the temperature gradient, it results in the melting of the polyethylene at the contact area, so that pseudo-liquid friction can occur. The temperature also promotes the adhesion of materials, when a roughness peak of the rollers interacts with polyethylene. It leads to the formation of numerous debris particles, and quasi similarity patterns for the polyetheretherketone PEEK-52100 - stainless steel pair were observed also by Laux et al. [50].

Table 2
Changes in tribological properties under dry machining conditions for minimum *Sa* compared to maximum *Sa*.

Parameters tested	Lubricating medium	
	Distilled water	SBF
f_{ch}	↑ 17%	↑ 11%
T	↑ 11%	↑ 4%
I_v	↑ 20%	↑ 21%

Table 3
Changes in tribological properties under MQL machining conditions for minimum *Sa* compared to maximum *Sa*.

Parameters tested	Lubricating medium	
	Distilled water	SBF
f_{ch}	↑ 4%	↑ 3%
T	~const	↑ 4%
I_v	↑ 2%	↓ 2%

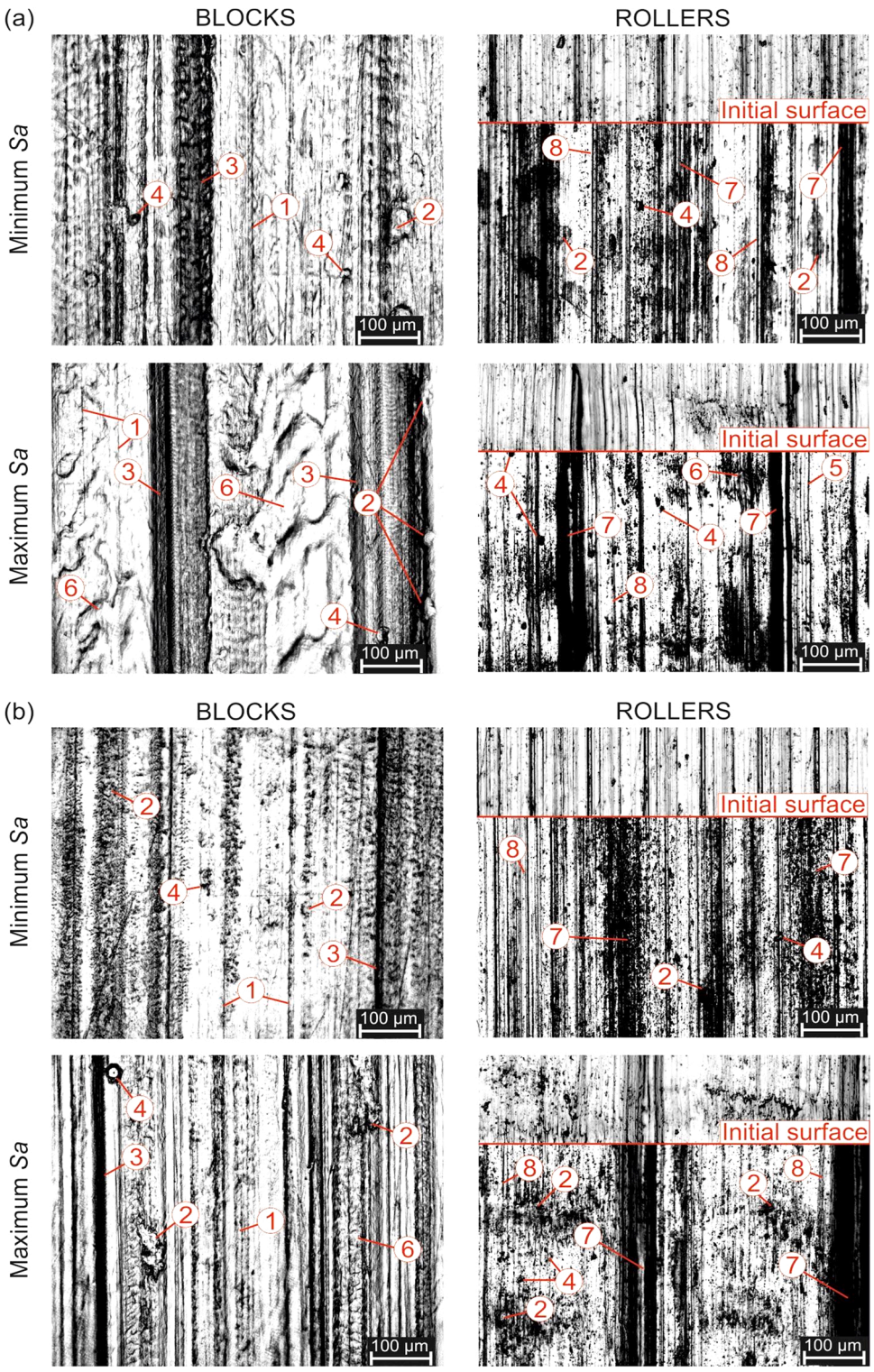

Fig. 7. Worn surfaces of samples and counter-bodies caused by friction in the presence of distilled water machined under (a) dry and (b) MQL conditions: 1 – abrasion tracks, 2 – adhesion areas, 3 – ploughing areas, 4 – debris particles, 5 – self-oscillation trails, 6 – melting areas, 7 – feed trails, 8 – turning trails.

Peaks on the roller surface in the form of feed ridges cause ploughing regardless of the rollers machining conditions and the type of lubricant. The presence of SBF intensifies the most of wear characteristics compared to distilled water. In fact, this can occur as an active reaction between anion and reactive metal surface [51]. Nevertheless, we have noted that the friction coefficient were slightly lower comparing to dry friction.

The mechanical and thermo-physical properties of the Ti6Al4V titanium alloy are much higher than those of UHMWPE, and therefore the wear of Ti6Al4V alloy rollers surfaces is negligible. The radial wear values measured with a high-resolution optimeter were of ~0.5 µm, i.e. 20% of the class 7 tolerance. The value were found almost the same over the whole wear cycle. However, polyethylene interacts actively with titanium alloy surfaces, as shown in Figs. 7 and 8. The major issue for long-term failure which leads to total joint replacement is associated to wear particles promoted by the UHMWPE as per Raffi and Srinivasan

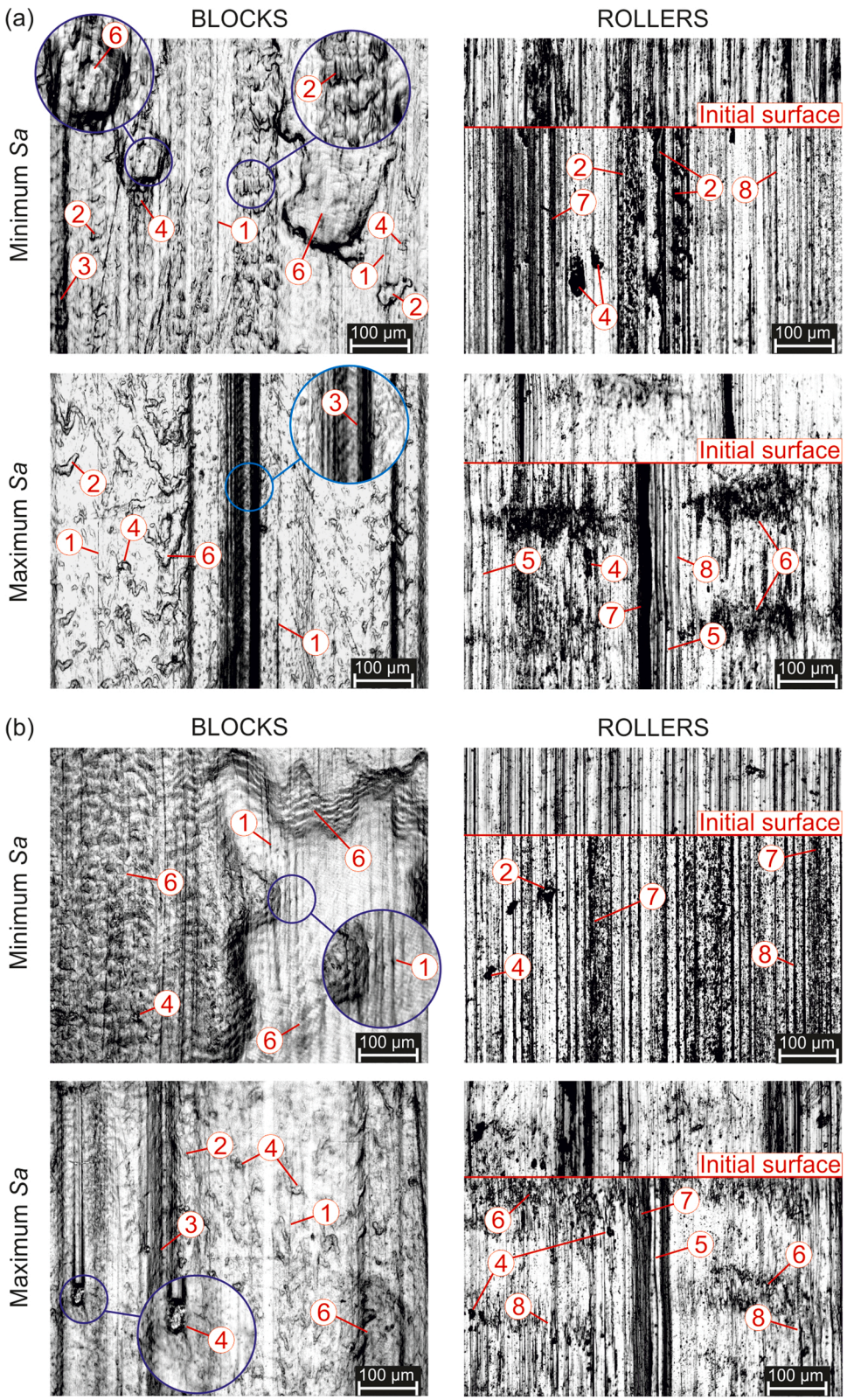

Fig. 8. Worn surfaces of samples and counter-bodies caused by friction in the presence of SBF machined under (a) dry and (b) MQL conditions: 1 – abrasion tracks, 2 – adhesion areas, 3 – ploughing areas, 4 – debris particles, 5 – self-oscillation trails, 6 – melting areas, 7 – feed trails, 8 – turning trails.

[52]. During friction in the presence of distilled water and SBF at low surface roughness and for dry and MQL machining conditions on UHMWPE surfaces, both adhesion joints and debris particles are observed. Additionally, there are melting areas in the presence of SBF. Compared to MQL cooling method, larger wear areas are observed on UHMWPE surfaces cooperating with the surface of Ti6Al4V alloy after dry cutting. Whereas, at high surface roughness only debris particles and melting areas are observed. On UHMWPE surfaces, larger melting areas are observed in the area of contact with the Ti6Al4V alloy surface for the dry cutting, while in the area of contact with the surface machined with

MQL method, greater amounts of debris particles. At the same time, traces of feeding and waviness caused by self-excited oscillations are observed on the rollers surface formed by finish turning, which was confirmed by the studied carried out by Leksycki and Feldshtein [45]. The similar influence of surface roughness was reported by Borjali et al. [53] and Nakanishi et al. [54]. No significant differences were observed on the worn surfaces of the Ti6Al4V alloy between the lubricants used in the tests, namely distilled water and SBF.

4. Conclusions

In this research were focused to detect the effects of surface topography as well as processing and environment conditions on tribological characteristics, especially momentary friction coefficient, temperature and wear rate of "Ti6Al4V alloy used against UHMWPE" friction pairs. The evaluation was performed on samples made of polyethylene with constant surface roughness and titanium alloy counter-bodies produced using finish turning under different conditions, with appropriate futures for human and the environment (dry and MQL) leading to different roughness of surface. Distilled water and simulated body fluid (SBF) were used as environment for the tribological trials conducted in this study. The following summary conclusions were found:

- Under dry and MQL machining conditions we achieved using minimum *Sa* a mixed directionally nature of the machined surface peaks while the maximum *Sa* triggered a periodic nature.
- The surfaces with maximum *Sa* values are characterized by sharp ridges, while surfaces with minimum *Sa* values are characterized by deeper valleys (especially for dry cutting). In addition, the surface with the minimum value of the *Sa* parameter after dry cutting is characterized by an increased number of sharp peaks compared to the surface after MQL conditions.
- The maximum *Sa* values provided more favorable results in respect to minimum *Sa* values. It is found that by using either distilled water or SBF some changes occur but they are marginal. Their tribological parameters do not exceed 21% and 4% using dry and MQL methods, respectively.
- Both for distilled water and SBF a lower momentary coefficient of friction and temperature have been recorded for dry-machined rollers, while less wear rate was observed for rollers processed under MQL conditions.
- Regardless of processing conditions and lubricant type, the main wear mechanisms of polyethylene were found as abrasion, adhesion and ploughing. The presence of debris and melting areas were also noticed. No wear was observed under titanium alloy analyzed, which can provide long-term and stable friction conditions on worn surfaces debris. However, small areas of polyethylene adhesion without significant changes in surface texture were observed.
- The type of lubricant practically does not affect the wear of the titanium alloy. Under dry and MQL machining conditions, on the samples with smaller surface roughness the wear may leads to the adhesion and formation of polyethylene particles on the titanium sample surface, whereas on the samples surfaces with a higher roughness the adhesion is not observed.
- The obtained research results are extremely important from the point of view of the designing of new biomedical components used for human implants produced by finishing turning.

Declaration of Competing Interest

The authors declare that they have no known competing financial interests or personal relationships that could have appeared to influence the work reported in this paper.

Acknowledgements

The authors gratefully acknowledge the financial support from the program of the Polish Minister of Science and Higher Education under the name "Regional Initiative of Excellence" in 2019 - 2022, project no. 003/RID/2018/19, funding amount 11 936 596.10 PLN".

References

[1] Teoh SH. Fatigue of biomaterials: a review. Int J Fatigue 2000;22:825–37. https://doi.org/10.1016/S0142-1123(00)00052-9.
[2] E SF, Shi L, Guo ZG, Liu WM. The recent progress of tribological biomaterials. Biosurf Biotribol 2015;1:81–97. https://doi.org/10.1016/j.bsbt.2015.06.002.
[3] Choi M, Hong E, So J, Song S, Kim BS, Yamamoto A, et al. Tribological properties of biocompatible Ti–10W and Ti–7.5TiC–7.5W. J Mech Behav Biomed Mater 2014;30:214–22. https://doi.org/10.1016/j.jmbbm.2013.11.014.
[4] Geetha M, Singh AK, Asokamani R, Gogia AK. Ti based biomaterials, the ultimate choice for orthopaedic implants – a review. Mater Sci 2009;54:397–425. https://doi.org/10.1016/j.pmatsci.2008.06.004.
[5] Temenoff J.S., Mikos A.G.: Biomaterials: The Intersection of Biology and Materials Science. Pearson-Prentice Hall, New Jersey, 2008.
[6] Chen Q, Thouas GA. Metallic implant biomaterials. Mater Sci Eng R Rep 2015;87:1–57. https://doi.org/10.1016/j.mser.2014.10.001.
[7] Papageorgiou I, Shadrick V, Davis S, Hails L, Schins R, Newson R, et al. Macrophages detoxify the genotoxic and cytotoxic effects of surgical cobalt chrome alloy particles but not quartz particles on human cells in vitro. Mutat Res Fund Mol M 2008;643:11–9. https://doi.org/10.1016/j.mrfmmm.2008.05.004.
[8] Goodman SB. Wear particles, periprosthetic osteolysis and the immune system. Biomaterials 2007;28:5044–8. https://doi.org/10.1016/j.biomaterials.2007.06.035.
[9] Sargeant A, Goswami T. Hip implants: Paper V. Physiological effects. Mater Des 2006;27:287–307. https://doi.org/10.1016/j.matdes.2004.10.028.
[10] Virtanen S, Milosev I, Gomez-Barrena E, Trebse R, Salo J, Konttinen YT. Special modes of corrosion under physiological and simulated physiological conditions (review). Acta Biomater 2008;4:468–76. https://doi.org/10.1016/j.actbio.2007.12.003.
[11] Wang Y, Shi LL, Duan DL, Li S, Xu J. Tribological properties of Zr61Ti2Cu25Al12 bulk metallic glass under simulated physiological conditions. Mater Sci Eng C 2014;37:292–304. https://doi.org/10.1016/j.msec.2014.01.016.
[12] Reisel G, Dorner-Reisel A. Hydrogen containing DLC coatings on UHMW-PE deposited by r.f.-PECVD. Diam Relat Mater 2007;16(4–7):1370–3. https://doi.org/10.1016/j.diamond.2006.11.095.
[13] Petrica M, Duscher B, Koch T, ArchodoulakiV M. Tribological investigations on virgin and accelerated aged PE-UHMW. Tribol Int 2015;87:151–9. https://doi.org/10.1016/j.triboint.2015.02.024.
[14] Barzegar M, Hashemi SJ, Nazokdast H, Karimi R. Evaluating the draft force and soil-tool adhesion of a UHMW-PE coated furrower. Soil Res 2016;163:160–7. https://doi.org/10.1016/j.still.2016.05.016.
[15] Arkusz K, Nycz M, Paradowska E. Electrochemical evaluation of the compact and nanotubular oxide layer destruction under ex vivo Ti6Al4V ELI transpedicular screw implantation. Materials 2020;13(1):1–16. https://doi.org/10.3390/ma13010176.
[16] Sartori S, Ghiotti A, Bruschi S. Temperature effects on the Ti6Al4V machinability using cooled gaseous nitrogen in semi-finishing turning. J Manuf Process 2017;30:187–94. https://doi.org/10.1016/j.jmapro.2017.09.025.
[17] Imbrogno S, Sartori S, Bordin A, Bruschi S, Umbrello D. Machining simulation of Ti6Al4V under dry and cryogenic conditions. Procedia CIRP 2017;58:475–80. https://doi.org/10.1016/j.procir.2017.03.263.
[18] McGee MA, Howie DW, Costi K, Haynes DR, Wildenauer CI, Pearcy MJ, et al. Implant retrieval studies of the wear and loosening of prosthetic joints: a review. Wear 2000;241:158–65. https://doi.org/10.1016/S0043-1648(00)00370-7.
[19] Chen J, Zhang Q, Li QA, Fu SL, Wang JZ. Corrosion and tribocorrosion behaviors of AISI 316 stainless steel and Ti6Al4V alloys in artificial seawater. Trans Nonferrous Met Soc 2014;24:1022–31. https://doi.org/10.1016/S1003-6326(14)63157-5.
[20] Sonekar M, Rathod WS. An experimental investigation on tribologial behavior of bio-implant material (SS-316 l & Ti6Al4V) for orthopaedic applications. Mater Today 2019;19(2):444–7. https://doi.org/10.1016/j.matpr.2019.07.633.
[21] Bruschi S, Bertolini R, Medea F, Ghiotti A. Influence of the machining parameters and cooling strategies the wear behavior of wrought and additive manufactured Ti6Al4V for biomedical applications. Tribol Int 2016;102:133–42. https://doi.org/10.1016/j.triboint.2016.05.036.
[22] Choubey A, Basu B, Balasubramaniam R. Tribological behaviour of Ti-based alloys in simulated body fluid solution at fretting contacts. Mater Sci Eng, A 2004;379(1–2):234–9. https://doi.org/10.1016/j.msea.2004.02.027.
[23] Allen C, Bloyce A, Bell T. Sliding wear behaviour of ion implanted ultra high molecular weight polyethylene against a surface modified titanium alloy Ti-6Al-4V. Tribol Int 1996;29(6):527–34. https://doi.org/10.1016/0301-679X(95)00116-L.
[24] Arkusz K, Paradowska E, Nycz M, Krasicka-Cydzik E. Influence of thermal modification and morphology of TiO2 nanotubes on their electrochemical properties for biosensors applications. J Nanosci Nanotechnol 2018;18(5):3713–21. https://doi.org/10.1166/jnn.2018.14685.

[25] Bian YY, Zhou L, Zhou G, Jin ZM, Xin SX, Hua ZK, et al. Study on biocompatibility, tribological property and wear debris characterization of ultra-low-wear polyethylene as artificial joint materials. J Mech Behav Biomed Mater 2018;82:87–94. https://doi.org/10.1016/j.jmbbm.2018.03.009.
[26] Wang Y, Yin Z, Li H, Gao G, Zhang X. Friction and wear characteristics of ultrahigh molecular weight polyethylene (UHMWPE) composites containing glass fibers and carbon fibers under dry and water-lubricated conditions. Wear 2017;380–381:42–51. https://doi.org/10.1016/j.wear.2017.03.006.
[27] Barret TS, Stachowiak GW, Batchelor AW. Effect of roughness and sliding speed on the wear and friction of ultra-high molecular weight polyethylene. Wear 1992;153(1):331–50. https://doi.org/10.1016/0043-1648(92)90174-7.
[28] Xiong D, Gao Z, Jin Z. Friction and wear properties of UHMWPE against ion implanted titanium alloy. Surf Coat Technol 2007;201(15):6847–50. https://doi.org/10.1016/j.surfcoat.2006.09.043.
[29] Langhorn J, Borjali A, Hippensteel E, Nelson W, Raeymaekers B. Microtextured CoCrMo alloy for use in metal-on-polyethylene prosthetic joint bearings: Multi-directional wear and corrosion measurements. Tribol Int 2018;124:178–83. https://doi.org/10.1016/j.triboint.2018.04.007.
[30] Maruda RW, Wojciechowski S, Szczotkarz N, Legutko S, Mia M, Gupta MK, et al. Metrological analysis of surface quality aspects in minimum quantity cooling lubrication. Measurement 2021;171:108847. https://doi.org/10.1016/j.measurement.2020.108847.
[31] Maruda RW, Feldshtein EE, Legutko S, Królczyk GM. Improving the efficiency of running-in for a bronze–stainless steel friction pair. J Frict Wear 2015;36(1):548–53. https://doi.org/10.3103/S1068366615060082.
[32] Yang J, Wang X, Kang M. Finite element simulation of surface roughness in diamond turning of spherical surfaces. J Manuf Process 2018;31:768–75. https://doi.org/10.1016/j.jmapro.2018.01.006.
[33] Sartori S, Bordin A, Ghiotti A, Bruschi S. Analysis of the surface integrity in cryogenic turning of Ti6Al4V produced by direct melting laser sintering. Procedia CIRP 2016;45:123–6. https://doi.org/10.1016/j.procir.2016.02.328.
[34] Zhang P, Liu Z. Modeling and prediction for 3D surface topography in finish turning with conventional and wiper inserts. Measurement 2016;94:37–45. https://doi.org/10.1016/j.measurement.2016.07.080.
[35] Sun J, Huang S, Wang T, Chen W. Research on surface integrity of turning titanum alloy TB6. Procedia CIRP 2018;71:484–9. https://doi.org/10.1016/j.procir.2018.05.028.
[36] Sun Y, Huang B, Puleo DA, Jawahir IS. Enhanced machinability of Ti-5553 alloy from cryogenic machining: comparison with MQL and flood-cooled machining and modeling. Procedia CIRP 2015;31:477–82. https://doi.org/10.1016/j.procir.2015.03.099.
[37] Krolczyk GM, Maruda RW, Krolczyk JB, Wojciechowski S, Mia M, Nieslony P, et al. Ecological trends in machining as a key factor in sustainable production – a review. J Clean Prod 2019;218:601–15. https://doi.org/10.1016/j.jclepro.2019.02.017.
[38] Statnikov RB, Statnikov AR. The Parameter Space Investigation Method Toolkit. Boston: Artech House; 2011.
[39] Krolczyk GM, Maruda RW, Krolczyk JB, Nieslony P, Wojciechowski S, Legutko S. Parametric and nonparametric description of the surface topography in the dry and MQCL cutting conditions. Measurement 2018;121:225–39. https://doi.org/10.1016/j.measurement.2018.02.052.
[40] Czifra A, Baranyi I. Sdq-Sdr topological map of surface topographies. Front Mech Eng 2020;6:1–9. https://doi.org/10.3389/fmech.2020.00050.
[41] Hussein MA, Mohammed AS, Al-Aqeeli N. Wear characteristics of metallic biomaterials: a review. Materials 2015;8(5):2749–68. https://doi.org/10.3390/ma8052749.
[42] Baino F, Yamaguchi S. The use of simulated body fluid (SBF) for assessing materials bioactivity in the context of tissue engineering: review and challenges. Biomimetics 2020;5(4):57. https://doi.org/10.3390/biomimetics5040057.
[43] Asri RIM, Harun WSW, Samykano M, Lah NAC, Ghani SAC, Tarlochan F, et al. Corrosion and surface modification on biocompatible metals: a review. Mater Sci Eng C 2017;77:1261–74. https://doi.org/10.1016/j.msec.2017.04.102.
[44] Dyachkova LN, Feldshtein EE, Vityaz' PA. Tribological behavior of sintered tin bronze with additions of alumina and nickel oxide. J Frict Wear 2013;34(1):19–26. https://doi.org/10.3103/S1068366613010042.
[45] Leksycki K, Feldshtein E. The surface texture of Ti6Al4V titanium alloy under wet and dry finish turning conditions. In: Królczyk G, Niesłony P, Królczyk J, editors. Industrial Measurements in Machining, Lecture Notes in Mechanical Engineering. Cham: Springer; 2020. p. 33–44. https://doi.org/10.1007/978-3-030-49910-5_4.
[46] Bordin A, Sartori S, Bruschi S, Ghiotti A. Experimental investigation on the feasibility of dry and cryogenic machining as sustainable strategies when turning Ti6Al4V produced by additive manufacturing. J Clean Prod 2017;142:4142–51. https://doi.org/10.1016/j.jclepro.2016.09.209.
[47] Niemczewska-Wójcik M. The influence of the surface geometric structure on the functionality of implants. Wear 2011;271:596–603. https://doi.org/10.1016/j.wear.2010.06.013.
[48] Baena J-C, Peng Z. Mechanical and tribological performance of UHMWPE influenced by temperature change. Polym Test 2017;62:102–9. https://doi.org/10.1016/j.polymertesting.2017.06.017.
[49] Dong G-N, Hua M, Li J, Chuah KB. Temperature field and wear prediction for UHMWPE acetabular cup with assumed rectangular surface texture. Mater Des 2007;28(9):2402–16. https://doi.org/10.1016/j.matdes.2006.09.015.
[50] Laux KA, Jean-Fulcrand A, Sue HJ, Bremner T, Wong JSS. The influence of surface properties on sliding contact temperature and friction for polyetheretherketone (PEEK). Polymer 2016;103:397–404. https://doi.org/10.1016/j.polymer.2016.09.064.
[51] Nycz M, Paradowska E, Arkusz K, Pijanowska DG. Influence of geometry and annealing temperature in argon atmosphere of TiO2 nanotubes on their electrochemical properties. Acta Bioeng Biomech 2020;22(1):165–77. https://doi.org/10.37190/ABB-01479-2019-03.
[52] Raffi NM, Srinivasan V. A study on wear behavior of γ-UHMWPE sliding against 316L stainless steel counter face. Wear 2013;306(1–2):22–6. https://doi.org/10.1016/j.wear.2013.06.023.
[53] Borjali A, Monson K, Raeymaekers B. Friction between a polyethylene pin and a microtextured CoCrMo disc, and its correlation to polyethylene wear, as a function of sliding velocity and contact pressure, in the context of metal-on-polyethylene prosthetic hip implants. Tribol Int 2018;127:568–74. https://doi.org/10.1016/j.triboint.2018.07.005.
[54] Nakanishi Y, Nakashima Y, Fujiwara Y, Komohara Y, Takeya M, Miura H, et al. Influence of surface profile of Co-28Cr-6Mo alloy on wear behaviour of ultra-high molecular weight polyethylene used in artificial joint. Tribol Int 2018;118:538–46. https://doi.org/10.1016/j.triboint.2017.06.030.